Measurement of the tensor analyzing power component T_{20} for the incoherent neutral-pion photoproduction on a deuteron

B. I. Vasilishin,[1] A. I. Fix,[1] V. V. Gauzshtein,[2,*] E. M. Darwish,[3,4] M. Ya. Kuzin,[1] M. I. Levchuk,[5] A. Yu. Loginov,[6] D. M. Nikolenko,[7] I. A. Rachek,[7] Yu. V. Shestakov,[7,8] D. K. Toporkov,[7,8] A. V. Yurchenko,[7] S. A. Zevakov,[7] A. V. Bogomyagkov,[7] A. N. Zhuravlev,[7] S. E. Karnaev,[7] V. A. Kiselev,[7] E. B. Levichev,[7] O. I. Meshkov,[7] S. I. Mishnev,[7] I. N. Okunev,[7] P. A. Piminov,[7] E. A. Simonov,[7] S. V. Sinyatkin,[7] and E. V. Starostina[7]

[1]*National Research Tomsk Polytechnical University, 634050 Tomsk, Russia*
[2]*Institute of High Current Electronics, 634055 Tomsk, Russia*
[3]*Physics Department, Faculty of Science, Taibah University, Medina 41411, Saudi Arabia*
[4]*Physics Department, Faculty of Science, Sohag University, Sohag 82524, Egypt*
[5]*Stepanov Institute of Physics, National Academy of Sciences of Belarus, 220072 Minsk, Belarus*
[6]*Tomsk State University of Control Systems and Radioelectronics, 634050 Tomsk, Russia*
[7]*Budker Institute of Nuclear Physics, 630090 Novosibirsk, Russia*
[8]*Novosibirsk State University, 630090 Novosibirsk, Russia*

(Received 6 May 2022; accepted 9 August 2022; published 18 August 2022)

The paper contains new results for the T_{20} component of the tensor analyzing power measured for the incoherent photoproduction of neutral pions on a deuteron, $\gamma d \to \pi^0 pn$. The results are presented for photon energies E_γ in the range from 300 to 600 MeV. The experimental statistics accumulated at the VEPP-3 accelerator complex in 2013 was used. To identify the events, the proton and two γ's from the $\pi^0 \to 2\gamma$ decay were registered in coincidence. For determination of T_{20}, the asymmetry of the reaction yield associated with the sign change of the tensor polarization of the deuterium target was measured. The experimental results are compared with theoretical calculations based on the spectator model, including interaction of the final state particles.

DOI: 10.1103/PhysRevC.106.024003

I. INTRODUCTION

Despite significant advances in hadronic physics in recent decades, development of the nonperturbative QCD methods still remains one of the most complicated and serious problems in this field. Due to the lack of a practically applicable fundamental theory for hadronic reactions in the low-energy regime, various phenomenological models are used based on the methods of quantum scattering theory in combination with the elements of relativistic quantum mechanics, current algebra, constituent quark models, etc. The phenomenological nature of such a theoretical framework obviously limits its predictive power. As a rule, different models give similar results only for a limited set of observables (basically those included into the fitted data set), whereas their predictions for other observables may differ significantly. Therefore, to achieve a unified description, it is very important to have the widest possible set of experimental data, which would ensure the convergence of various model calculations. The ideal case is a data set providing a complete experiment, which would allow, at least in principle, the determination of the reaction amplitudes without relying on model assumptions.

Recently, a noticeable step forward was made in meson photoproduction on nucleons and nuclei thanks to a new generation of single and double polarization experiments. In particular, a large amount of new precise data have been accumulated by the Crystal Ball Collaboration at MAMI, CLAS at JLab, as well as in the CBELSA/TAPS experiments in Bonn. The data obtained have a significant impact on the existing partial wave analyzes. In general, successive fitting of various models to new data demonstrates clear convergence of the resulting solutions for multipole amplitudes. Thus, one can hope that further accumulation of the data will gradually make it possible to achieve the final goal: construction of a unique model-independent multipole analysis.

Violation of the isospin symmetry in electromagnetic transitions requires measurement of photoproduction on both protons and neutrons. In this case, the quasifree reaction, $\gamma d \to \pi NN$, in which the deuteron acts as an effective neutron target, acquires special significance. One can note a fairly large number works in this area (a comprehensive review can be found, e.g., in [1]) in which the weak binding of nucleons in the deuteron is exploited as a decisive factor in extracting polarization observables on the neutron. It should also be noted that various nuclear effects such as Fermi motion, presence of the D state in the deuteron wave function, the Pauli exclusion principle, etc. tend to cancel out in the ratio of the polarized to the unpolarized cross section, so that the resulting asymmetry is to a large extent free from various model uncertainties.

Moreover, the study of polarization observables for photoproduction on the deuteron is interesting in itself. In particular,

*gauzshtein@tpu.ru

since the structure of the deuteron is well understood, this process becomes an ideal testing tool for different models under controlled conditions. To date, there are quite a large number of experimental and theoretical works [2–13] devoted to a detailed study of these reactions. Furthermore, in recent years, a global program of experiments for measuring polarization observables in electromagnetic processes on deuterons has been developed at various electron accelerators and laser backscattering facilities. A comprehensive review of the current state of such experiments may be found, e.g., in Ref. [14].

In this work, we present new results for the tensor analyzing power component T_{20} obtained for incoherent neutral-pion photoproduction on a deuteron, $\gamma d \to \pi^0 pn$. To date, experimental studies of photonuclear reactions on tensor-polarized deuterons have been carried out only on the internal tensor-polarized deuterium target at the VEPP-3 accelerator complex [15–24]. The data obtained in the 2003 experiment provided the first results on the components T_{2M} for the coherent $\gamma d \to \pi^0 d$ [19,24] channel as well as the incoherent $\gamma d \to \pi^0 pn$ [21–23] channel. Unfortunately, the statistical accuracy of these results was rather low, since the main purpose was to study the role of tensor forces in deuteron photodisintegration [20].

In the present study we use the experimental statistics for the reaction $\gamma d \to \pi^0 pn$ accumulated at VEPP-3 in 2013. Unlike the previous measurements, the main goal of the last experiment was to study the coherent π^0 photoproduction on a tensor-polarized deuterium target using an unpolarized photon beam [25–29]. In contrast to the experiment of 2003, in which only two final nucleons were detected, in the present case the proton and two γ quanta from the $\pi^0 \to 2\gamma$ decay were detected in coincidence.

The paper is organized as follows. In the next two sections the experimental setup and some important details of the data analysis are described. In Sec. IV, the experimental data are presented and compared with a statistical simulation based on the model of Ref. [6]. Finally, in Sec. V we summarize our results.

II. EXPERIMENTAL SETUP

In the present experiment, the pions were produced by the incoherent electron scattering $ed \to e'\pi^0 pn$. The polar angle of the scattered electrons was close to zero for the major part of the events. To estimate the value of the momentum transfer squared, we used the $ed \to e'\pi^0 pn$ data from Ref. [30]. The mean value thus found is very small, about 0.0025 $(\mathrm{GeV}/c)^2$, so the longitudinal polarization of virtual photons can be neglected, and the incident photon beam can be treated as quasireal photons.

The main goal of the experiment was to study the π^0 photoproduction in the coherent channel, $\gamma d \to \pi^0 d$. At the same time, determination of the kinematic parameters of two γ's from the $\pi^0 \to 2\gamma$ decay allows one to determine the kinematic parameters of the π^0 meson and thus to study the incoherent reaction $\gamma d \to \pi^0 pn$ as well.

In the absence of vector polarization of the deuteron target, the differential cross section of the incoherent π^0 photoproduction on a tensor polarized deuteron $\gamma d \to \pi^0 pn$ reads

$$d\sigma = d\sigma_0 \Big\{ 1 + \frac{1}{\sqrt{2}} P_{zz} \big[d^2_{00}(\theta_H)\, T_{20} + d^2_{10}(\theta_H)\, \cos\phi_H T_{21} + d^2_{20}(\theta_H)\, \cos 2\phi_H T_{22} \big] \Big\}, \quad (1)$$

where $d\sigma_0$ is the corresponding unpolarized cross section, and $d^M_{IM}(\theta_H)$ are the Wigner d functions:

$$d^2_{00}(\theta_H) = \frac{3}{2}\cos^2\theta_H - \frac{1}{2},$$
$$d^2_{10}(\theta_H) = \sqrt{\frac{3}{8}}\sin 2\theta_H,$$
$$d^2_{20}(\theta_H) = \sqrt{\frac{3}{8}}\sin^2\theta_H. \quad (2)$$

The factors T_{20}, T_{21}, and T_{22} in Eq. (1) are the components of the tensor analyzing power of the reaction $\gamma d \to \pi^0 pn$, P_{zz} is the degree of tensor polarization of the deuteron target, and the angles θ_H and ϕ_H determine the orientation of the magnetic field in the coordinate system with the z axis along the initial photon momentum.

The tensor polarization P_{zz} can be expressed in terms of the populations n^S of the deuteron states with the spin projections $S = -1, 0, +1$ on the direction of the magnetic field:

$$P_{zz} = 1 - 3n^0 = 3(n^+ + n^-) - 2. \quad (3)$$

In the present experiment, the magnetic field was directed along the photon beam, so that $\theta_H = 0$. This implies that in Eq. (1) only the T_{20} component contributes to the differential cross section. Note that Eq. (1) is valid only for coplanar kinematics, when the momenta of all three final particles (the two nucleons and the pion) span the same plane.

The component T_{20} was calculated according to

$$T_{20} = \sqrt{2}\frac{N^+ - N^-}{P^+_{zz}N^- - P^-_{zz}N^+}, \quad (4)$$

with N^+ (N^-) being the number of events for the tensor polarization of the deuteron target equal to P^+_{zz} (P^-_{zz}).

The general scheme of the experiment is shown in Fig. 1. The elements of the detector were placed in a vertical plane above and below the beam axis. To identify the $\gamma d \to pn\pi^0$ reaction, the events corresponding to the triple coincidences of a proton and two γ quanta from $\pi^0 \to \gamma\gamma$ were selected. The protons and the photons from the pion decay were detected by the upper and the lower arm of the detecting system, respectively.

The upper arm consisted of the drift chambers and three layers of plastic scintillators, 2, 12, and 20 cm thick, respectively. For the best timing performance, each scintillator was equipped with two photomultipliers, one at each end. The present results correspond to the protons stopped in the first, second, or third scintillator. The proton energy was in the region 20–180 MeV. The error of the energy determination was less than 12% for the protons stopped in the first scintillator and did not exceed 20% for the protons in the second and the third scintillators.

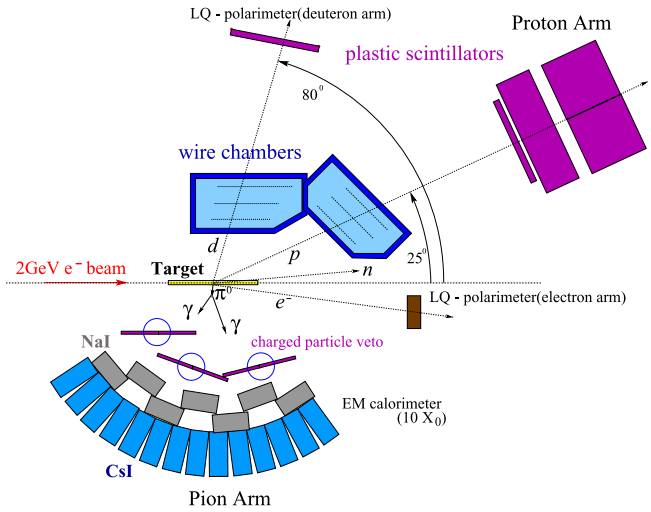

FIG. 1. The general scheme of the experimental setup.

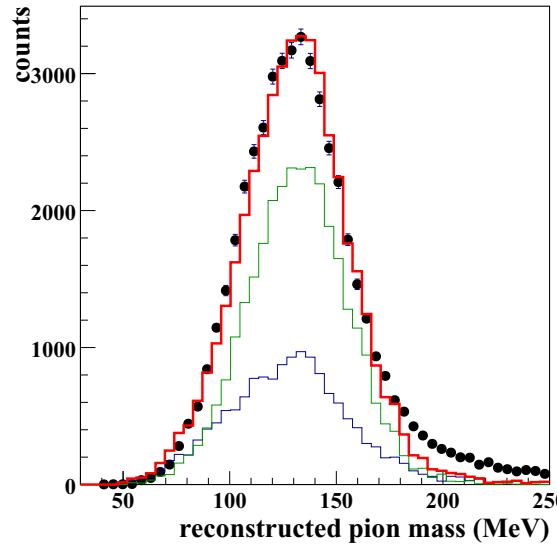

FIG. 2. Distribution of the reconstructed pion mass. The points correspond to the experimental data and the colored curves are the results of the GEANT4 simulation: the green curve corresponds to the reaction $\gamma d \to \pi^0 pn$, the blue curve corresponds to background reactions, and the red curve is the sum of the two curves.

The photons from the $\pi^0 \to \gamma\gamma$ decay were detected by a calorimeter consisting of a layer of NaI(Tl) blocks 5 cm thick and a layer of CsI(Tl) blocks 15 cm thick. The blocks were used in a number of other experiments at VEPP-3. A detailed description of their design and characteristics can be found in Ref. [31]. The total radiation length of the calorimeter was $10.0X_0$. The scintillation light from the NaI(Tl) crystals was detected by photomultiplier tubes. These signals were then used in a hardware trigger with a threshold of 10 MeV. The scintillation light from the CsI(Tl) crystals was collected by wavelength-shifted plates and PIN silicon photodiodes. Thin plastic counters were installed in front of the NaI blocks to separate neutral and charged particles. The count rates at the maximum beam current were 4 and 130 kHz for the NaI layer and the charge veto layer, respectively. The corresponding count rate of the coincidence trigger was 200 Hz.

An open storage cell installed in the orbit of the VEPP-3 storage ring was used as an internal gas target. Tensor-polarized deuterons were injected into the center of the cell from an atomic beam source (ABS) installed in the median plane of VEPP-3 [32]. The target thickness was 3.5×10^{13} atoms/cm^2. The sign of the tensor polarization of the deuterium target changed every 30 seconds during the data taking. This duration is three orders of magnitude smaller than the typical target density change period, which is mainly due to the slow degradation of the ABS inner surfaces (see Ref. [32] for details). Thus, the false asymmetry associated with fluctuations in the target density was insignificant, and the absolute value of the target thickness is not required to calculate the asymmetries.

An additional pair of arms was used to detect elastically scattered electrons and recoil deuterons. The data collected by these detectors made it possible to measure the target polarization (the details can be found in Ref. [33]). The resulting run-averaged degrees of the tensor polarization were $P_{zz}^{+} = +0.42 \pm 0.02$ and $P_{zz}^{-} = -0.72 \pm 0.03$.

III. DATA ANALYSIS

To identify the events from the $\gamma d \to pn\pi^0$ reaction, the proton and the photons from the $\pi^0 \to \gamma\gamma$ decay were detected in coincidence. The condition for coincidence of the γ quanta was the loss of energy by two clusters in one event. A cluster is a collection of hits in the NaI(Tl) or CsI(Tl) crystals located next to each other. When the photon hits the calorimeter, all the energy is released in a limited volume—a cluster. A necessary condition for reconstruction of the π^0 kinematic parameters is the presence of two clusters in which energy is released. Another condition is the absence of a signal in the veto counter indicating a transit of an uncharged particle. The kinematic parameters of π^0 were reconstructed from the absorbed energy and the angle between two separated clusters. To identify the events corresponding to the π^0 detection, the pion mass was reconstructed from the data.

Figure 2 shows the experimental distribution of the reconstructed pion mass. There we have also plotted the corresponding distribution obtained by simulating the experiment using the GEANT4 [34] package together with the photoreaction generator GENBOS [35]. Fairly good agreement between the experiment and the simulation results indicates the correctness of the technique used for reconstructing the π^0 kinematical parameters. In the simulated distribution, a rather tangible (about 30%) contribution of the background reactions is well seen. It is basically due to the fact that the pion mass was reconstructed for all events in which two photons were detected. The reconstruction accuracy was not worse than 20 MeV.

To identify protons in the upper detector, we reconstructed the mass of a particle detected in one of the three plastic scintillators. The mass was determined using the time of flight from the target to the first scintillator and the energy loss in

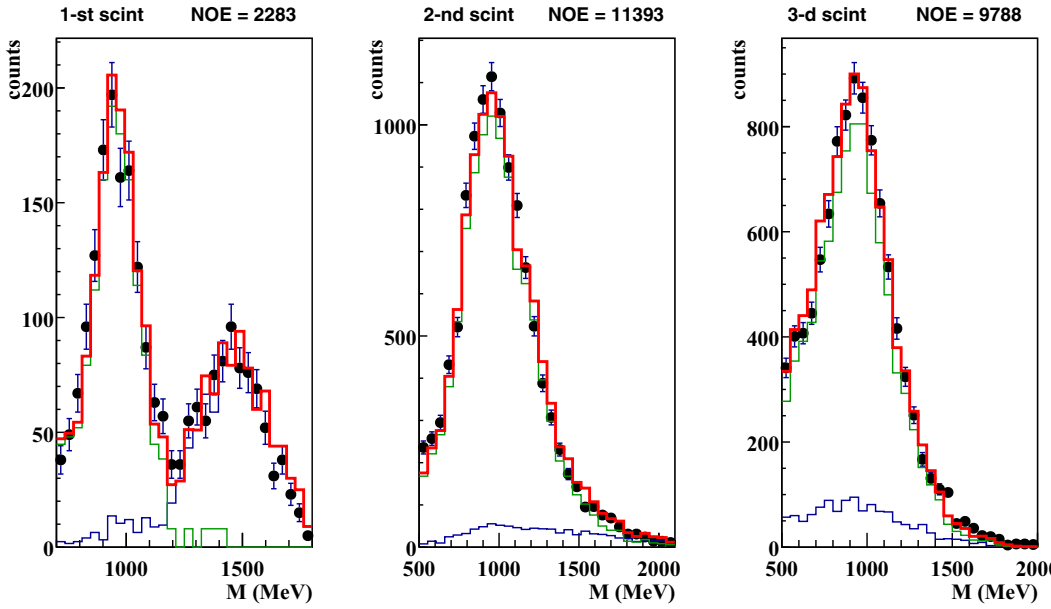

FIG. 3. Distribution of the reconstructed proton mass for the first (left panel), second (middle panel), and third (right panel) scintillators. Notations are as in Fig. 2.

the scintillator where the particle was stopped. For the start time for each event we took the time at which the electron bunch crosses the target. Taking into account the size of the electron bunch, the uncertainty of the start time was about 0.1 ns. The stop time was determined as the time of the signal coming from the first scintillator. Using GEANT4 simulation, the appropriate coefficients were obtained which convert the measurement time into the real time of flight from the target to the first scintillator.

In Fig. 3 we plot the distribution of the reconstructed proton mass for three plastic scintillators. The blue curves in this figure show the background contribution, which in our case comes mainly from the coherent channel $\gamma d \to \pi^0 d$, as well as from the double photoproduction process $\gamma d \to \pi^0\pi^0 np$. The role of the corresponding coherent reaction $\gamma d \to \pi^0\pi^0 d$ is insignificant because of anomalous smallness of its cross section. On the left panel, showing the mass distribution in the first scintillator, one can see the second maximum at about 1.45 GeV. This structure is due to the recoil deuterons coming from $\gamma d \to \pi^0 d$. Since the mass determination is calibrated for protons, it gives the correct position for the proton maximum, whereas the deuteron peak is shifted to lower energies.

As direct calculations show, in the kinematical region covered by our measurements, the energy of the deuterons produced in $\gamma d \to \pi^0 d$ is in the interval that basically coincides with the interval of deuteron detection in the first scintillator, 15–80 MeV. For this reason, the analogous "deuteron" peaks in the second and the third scintillators (the middle and right panels in Fig. 3) are practically invisible. Here, the major part of the background comes from the protons arising from the incoherent channel $\gamma d \to \pi^0\pi^0 np$.

In the lower arm, the events were selected for which the reconstructed π^0 mass was within 5σ. General agreement between the reconstructed mass obtained from the experimental data and that obtained by the GEANT4 simulation together with the GENBOS photoreaction generator made it possible to estimate the contribution of the background reactions to the selected experimental statistics. For events in which the proton was detected in the first, second, and third scintillators, the background contribution was 7.1%, 4.5%, and 9.3%, respectively.

The kinematics of the $\gamma d \to \pi^0 pn$ reaction was reconstructed from the measured γ and π^0 kinematic parameters. The scattered electron was not detected, but, as is known, with such an experimental setup, the polar angle of the electron is in most cases very close to zero, since the electroproduction cross section is strongly forward peaking due to the $1/Q^2$ dependence of the virtual photon flux. Taking the polar angle of the scattered electron equal to zero and measuring the emission angles and the energy of both the proton and the pion, one can completely restore the reaction kinematics.

IV. RESULTS AND DISCUSSION

For a complete systematic analysis of the experimental results for T_{20}, we compared them with the corresponding values obtained by statistic simulation of $\gamma d \to \pi^0 pn$. The simulation was carried out using the Monte Carlo algorithm proposed in Refs. [36,37], where the amplitude of the reaction $\gamma d \to \pi^0 pn$ is used. For consistency, the amplitude has to be built into the theoretical model, and be in fair agreement with the existing experimental data. For such a model, we took the one developed in Ref. [6]. It includes the quasifree photoproduction on a bound nucleon and takes into account πN and NN rescattering in the final state. For the elementary $\gamma N \to \pi N$ process the MAID2007 multipole analysis from [38] was adopted. For the deuteron wave function as well as for the final NN system we took the separable version of the Paris potential [39,40] with the NN partial waves up to $^3D_3$. As discussed in [6], the interaction between the final

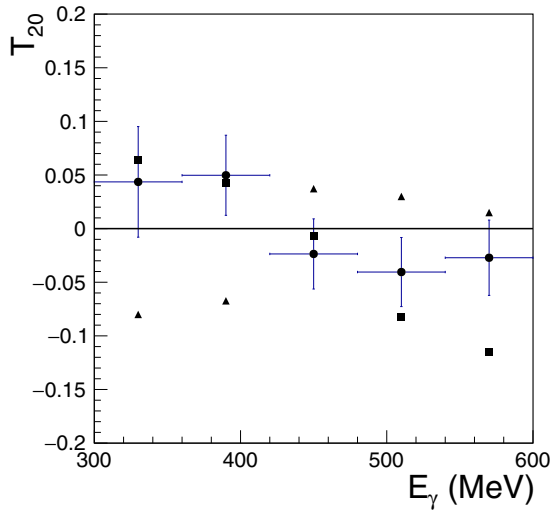

FIG. 4. Dependence of the tensor analyzing power component T_{20} of the reaction $\gamma d \to \pi^0 pn$ on the photon energy E_γ. The circles are the experimental results, the triangels are the results of simulation within the framework of impulse approximation, and the squares are the results of simulation taking into account the final state interaction.

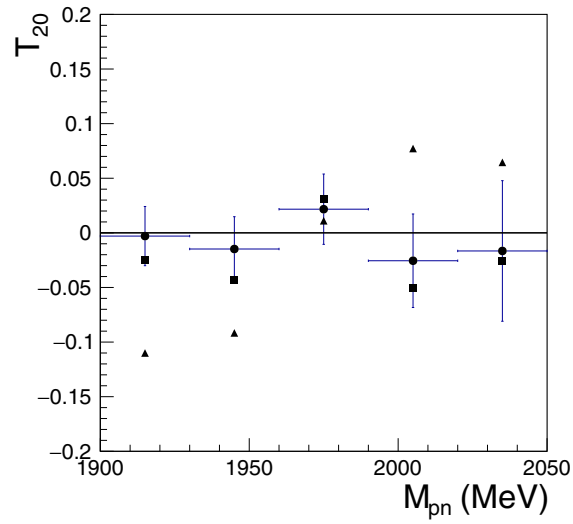

FIG. 5. Dependence of the tensor analyzing power component T_{20} of the reaction $\gamma d \to \pi^0 pn$ on the invariant proton-neutron mass M_{pn}. The notations are the same as in Fig. 4.

nucleons is of particular importance for the incoherent π^0 photoproduction on a deuteron. It results in about 20% reduction of the total cross section in the region of the $\Delta(1232)\,\frac{3}{2}^+$ resonance. Inclusion of the πN interaction leads to further reduction of the reaction yield. The latter effect is not so significant and can affect the cross section value only in a very limited region of the reaction phase space, as a rule, in the region associated with large transferred momenta. For the πN scattering amplitude we used the partial wave analysis of Ref. [41], including the waves up to $L = 2$.

Statistic simulation of the reaction allows direct comparison of the experimental data with the model predictions. As independent kinematic variables, we used the photon energy, the emission angles of the final neutron and proton, and the energy of the final proton. The energy distribution of the incident photons was simulated using the Dalitz spectrum [42]. After statistical sampling of six independent kinematic variables, the matrix elements of the reaction amplitude were calculated.

The differential cross section was obtained by convolving these matrix elements with the density matrix for the tensor polarized deuteron. The elements of the density matrix correspond to one of the two polarization states of the deuteron target with equal probability $P = 1/2$. After that, the Neumann method was applied for accepting or rejecting the reaction events. In total, 10^6 of the simulated events were selected, which is approximately two orders of magnitude larger than the number of the reaction events selected during the data handling. The tensor analyzing power component T_{20} was extracted from the simulated events in the same way as when using the real experimental events, thus making it possible to directly compare the experimental and the simulated results.

Our data for $\gamma d \to \pi^0 pn$ are presented in Figs. 4–6. For each data point, the total error derived from the statistical and the systematic errors, as the square root of the sum of their squares, is also presented. The main source of the systematic error in the present measurements is the uncertainty in the degree of the deuteron tensor polarization. Its contribution to the resulting total error is, however, insignificant because of a rather large statistical error of our data.

Figure 4 shows the experimental and simulated values of T_{20} as functions on the photon energy E_γ. The statistic simulation was performed using the model of [6] and the algorithm [36,37]. As can be seen from the figure, the measured T_{20} component agrees rather satisfactorily with the simulated values. The largest discrepancy is observed in the energy range $500 < E_\gamma < 600$ MeV, corresponding to the maximum photon energy. Figure 5 shows the dependence of the

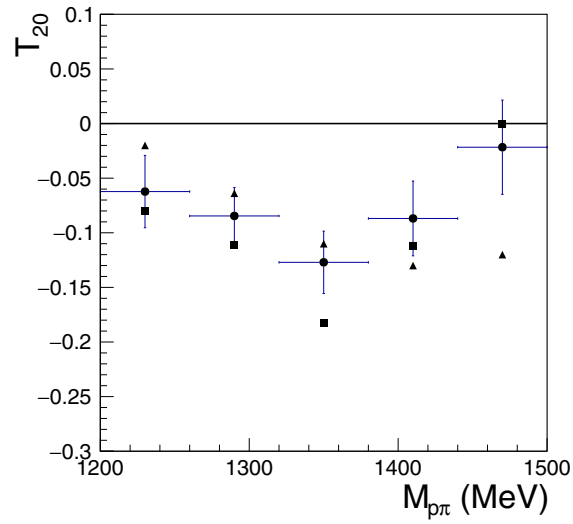

FIG. 6. Dependence of the tensor analyzing power component T_{20} of the reaction $\gamma d \to \pi^0 pn$ on the invariant pion-proton mass $M_{p\pi^0}$. The notations are the same as in Fig. 4.

measured T_{20} value on the invariant pn mass M_{pn} together with the results of statistic simulation. As we can see, the presented dependencies are in fair agreement over the entire range of M_{pn}.

Figure 6 also shows the experimental and the simulated dependencies of T_{20} on the proton-pion invariant mass $M_{p\pi^0}$. As in the previous cases, there is a satisfactory agreement between the experimental and model results. A noticeable discrepancy can be seen only in the region $1320 < M_{p\pi^0} < 1380$ MeV.

One can notice some difference in the mean values of T_{20} in Figs. 4, 5 and Fig. 6. Namely, it is close to zero in the first two figures, whereas in Fig. 6 it is shifted to about -0.06. This applies to both the experimental data and to the results of simulation. The difference is caused by rather strong sensitivity of the fraction in Eq. (4) to a specific partitioning of the same data set. The second reason is a slightly different number of events selected for the $M_{\pi p}$ distribution. In detail, while in Figs. 4 and 5 we used, respectively, 11779 and 11810 events, in Fig. 6 this number amounts to 12967. Since the statistic simulation was performed with the same partitioning of the events, the corresponding T_{20} values in Fig. 6 are also slightly shifted to the negative region.

Given the sensitivity of the presented results to the details of the reaction mechanism in our kinematical region, we can conclude that the agreement between experiment and statistic simulation is quite satisfactory. However, other possible mechanisms have to be taken into account to improve the agreement. The latter may include, for example, the interaction between the nucleon resonance and the spectator nucleon in the intermediate state, as well as the $\Delta\Delta$ component of the deuteron wave function [39] and additional contributions to the NN interaction which may be important at small internucleon distances [43–46].

V. SUMMARY

In this paper, we present the new results for the T_{20} component of the tensor analyzing power for incoherent π^0 photoproduction on a deuteron in the energy region $300 < E_\gamma < 600$ MeV. The experimental data are compared with the results of statistic simulation carried out using the $\gamma d \to \pi NN$ model of Ref. [6]. The latter includes photoproduction on a quasifree nucleon followed by πN and NN rescatterings in the final state. We find satisfactory agreement of the data with the simulation results.

Comparison with simulation demonstrates the essential role of the final state interactions in NN and πN subsystems. Inclusion of the interaction effects visibly improves the agreement with the data. It is therefore evident that any realistic description of T_{20} in the kinematical region considered requires careful treatment of these effects.

We have also discussed the experimental dependence of T_{20} on the proton-neutron and pion-proton invariant masses. According to our results, this dependence agrees satisfactorily with the statistic simulation, except for the range of the invariant pion-proton mass $1320 < M_{p\pi^0} < 1380$ MeV.

Some deviation between the model simulation and the data is seen in the region of high photon energies $E_\gamma > 500$ MeV. The interpretation of this discrepancy requires a detailed study of corrections to the simple spectator-participant description of the reaction mechanism. Perhaps the agreement between theory and experiment can be improved by taking into account the contribution of additional mechanisms to the amplitude.

ACKNOWLEDGMENT

The data analysis of this work was supported by the Russian Science Foundation, Grant No. 22-42-04401.

[1] W. J. Briscoe, A. E. Kudryavtsev, I. I. Strakovsky, V. E. Tarasov, and R. L. Workman, Eur. Phys. J. A **58**, 23 (2022).
[2] J. M. Laget, Phys. Rep. **69**, 1 (1981).
[3] R. Schmidt, H. Arenhövel, and P. Wilhelm, Z. Phys. A **355**, 421 (1996).
[4] I. T. Obukhovsky *et al.*, J. Phys. G **29**, 2207 (2003).
[5] V.E. Tarasov, W.J. Briscoe, H. Gao, A.E. Kudryavtsev, and I.I. Strakovsky, Phys. Rev. C **84**, 035203 (2011).
[6] A. Fix and H. Arenhövel, Phys. Rev. C **72**, 064005 (2005).
[7] E.M. Darwish, C. Fernandez-Ramirez, E. Moya de Guerra, and J.M. Udias, Phys. Rev. C **76**, 044005 (2007).
[8] M. I. Levchuk, Phys. Rev. C **82**, 044002 (2010).
[9] K. Helbing, Prog. Part. Nucl. Phys. **57**, 405 (2006).
[10] J. Ahrens *et al.*, Phys. Rev. Lett. **97**, 202303 (2006).
[11] J. Ahrens *et al.*, Phys. Lett. B **672**, 328 (2009).
[12] J. Ahrens *et al.*, Eur. Phys. J. A **44**, 189 (2010).
[13] B. Krusche, Acta Phys. Pol. B **51**, 61 (2020).
[14] See the IUPAP Report 41: A Worldwide Perspective Of Research And Research Facilities in Nuclear Physics by the IUPAP Working Group 9, http://www.iupap.org/wg/
[15] V. V. Gauzshtein *et al.*, Nucl. Phys. A **968**, 23 (2017).
[16] V. V. Gauzshtein *et al.*, Phys. At. Nucl. **78**, 1 (2015).
[17] V. V. Gauzshtein *et al.*, Russ. Phys. J. **59**, 868 (2016).
[18] V. N. Stibunov *et al.*, J. Phys.: Conf. Ser. **295**, 012115 (2011).
[19] D. M. Nikolenko *et al.*, JETP Lett. **89**, 432 (2009).
[20] I. A. Rachek *et al.*, Phys. Rev. Lett. **98**, 182303 (2007).
[21] S. E. Lukonin *et al.*, Int. J. Mod. Phys. E **28**, 1950010 (2019).
[22] S. E. Lukonin *et al.*, Russ. Phys. J. **62**, 252 (2019).
[23] S. E. Lukonin *et al.*, Nucl. Phys. A **986**, 75 (2019).
[24] I. A. Rachek *et al.*, J. Phys.: Conf. Ser. **295**, 012106 (2011).
[25] S. A. Zevakov *et al.*, Bull. Russ. Acad. Sci. Phys. **78**, 611 (2014).
[26] S. A. Zevakov *et al.*, Bull. Russ. Acad. Sci. Phys. **79**, 864 (2015).
[27] I. A. Rachek *et al.*, Few-Body Syst. **58**, 29 (2017).
[28] V. V. Gauzshtein *et al.*, Eur. Phys. J. A **56**, 169 (2020).
[29] V. V. Gauzshtein *et al.*, Int. J. Mod. Phys. E **29**, 2050011 (2020).
[30] M. Tammam, A. Fix, and H. Arenhovel, Phys. Rev. C **74**, 044001 (2006).
[31] J. A. P. Theunissen *et al.*, Nucl. Instrum. Methods Phys. Res., Sect. A **348**, 61 (1994).
[32] M. V. Dyug *et al.*, Nucl. Instrum. Methods Phys. Res., Sect. A **495**, 8 (2002).

[33] M. V. Dyug *et al.*, Nucl. Instrum. Methods Phys. Res., Sect. A **536**, 344 (2005).
[34] S. Agostinelli *et al.*, Nucl. Instrum. Methods Phys. Res., Sect. A **506**, 250 (2003).
[35] A. S. Iljinov *et al.*, Nucl. Phys. A **616**, 575 (1997).
[36] G. I. Kopylov, Zh. Exp. Teor. Fiz. **35**, 1426 (1958) [Sov. Phys. JETP **8**, 996 (1959)].
[37] G. I. Kopylov, Zh. Exp. Teor. Fiz. **39**, 1091 (1960) [Sov. Phys. JETP **12**, 761 (1961)].
[38] D. Drechsel, S. Kamalov, and L. Tiator, Eur. Phys. J. A **34**, 69 (2007)
[39] J. Haidenbauer and W. Plessas, Phys. Rev. C **30**, 1822 (1984).
[40] J. Haidenbauer and W. Plessas, Phys. Rev. C **32**, 1424 (1985).
[41] S. Nozawa *et al.*, Nucl. Phys. A **513**, 459 (1990).
[42] R. H. Dalitz and D. R. Yennie, Phys. Rev. **105**, 1598 (1957).
[43] Yu. F. Smirnov and Yu. M. Tchuvilsky, J. Phys. G **4**, L1 (1978).
[44] V. I. Kukulin *et al.*, J. Phys. G **27**, 1851 (2001).
[45] V.I. Kukulin, I.T. Obukhovsky, P. Grabmayr, and A. Faessler, Phys. Rev. C **74**, 064005 (2006).
[46] V. I. Kukulin *et al.*, Eur. Phys. J. A **56**, 229 (2020).